I&EC research
Industrial & Engineering Chemistry Research

pubs.acs.org/IECR

Article

Azeotropic Refrigerant Mixture R-513A Separation Using Extractive Distillation with Ionic Liquids Entrainers

Abdulrhman M. Arishi and Mark B. Shiflett*

Cite This: *Ind. Eng. Chem. Res.* 2023, 62, 19862−19872

Read Online

ACCESS | Metrics & More | Article Recommendations | Supporting Information

ABSTRACT: Hydrofluoroolefins (HFOs) are the next generation of refrigerants that have significantly lower global warming potential (GWP) and zero ozone-depleting potential (ODP) and will function as a replacement for hydrofluorocarbons (HFCs). During the transition to HFO refrigerants, a blend of HFC and HFO will be used to reduce the GWP and provide thermophysical properties that are suitable for use in replacing HFCs in existing equipment that may not be compatible or operating with the same performance with only HFOs. The formation of azeotropes in HFC/HFO blends poses a challenge when recycling and reclaiming the refrigerant. To address the problem of azeotropic mixture separation, a highly efficient separation method is required. Extractive distillation using an ionic liquid (IL) as an entrainer is proposed, offering effective separation of azeotropic mixtures. The effectiveness of ILs as an entrainer was determined by selectivity and high affinity toward one or more components of the mixture. The proper selection of the IL as an entrainer for a particular gas mixture is dictated by the purity of the products and the energy and cost of separation. Nine ILs were individually simulated in an equilibrium-based model to separate R-513A using ASPEN Plus to compare the impact of solvent choice on the separation cost. The ILs exhibited variations in overall heat duties, number of stages (N_T), operating pressure (P), solvent to feed ratio (S/F), and reflux ratio (RR). The best entrainer option for the separation of R-513A was found to be 1-ethyl-3-methylimidazolium acetate.

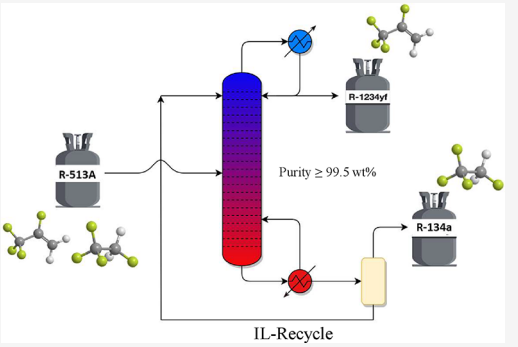

1. INTRODUCTION

Over the past several decades, hydrofluorocarbon (HFC) refrigerants have been used as a replacement for hydrochlorofluorocarbon (HCFC) and chlorofluorocarbon (CFC) refrigerants. HFCs are nonozone-depleting potential (ODP) refrigerants but have relatively high global warming potentials (GWP).[1] Some HFCs commonly used in air-conditioning and refrigeration systems are considered potent greenhouse gases (GHGs) and are now an environmental concern. The Kigali Amendment to the Montreal Protocol is an international agreement that mandates all countries to phase down the production and consumption of HFCs and recommends that the industry develop new alternatives with the same performance and minimal impact on the environment.[2] European regulation (EU) no. 517/2014 (The European Parliament and the Council of the European Union, 2014) has banned refrigerants with a GWP greater than 2500 and refrigerants that contain HFCs with a GWP greater than 150 for domestic use since January 1st, 2015[3] to encourage the refrigerant industry to develop alternatives that have minimal impact on the environment. In the U.S., the American Innovation and Manufacturing (AIM) Act proposes to phase down the consumption and production of HFCs with high GWP by 85% within the next 15 years.[4] A revolutionary transition in the refrigerant industry is occurring with the introduction of the next generation of refrigerants, hydrofluoroolefins (HFOs). HFOs are unsaturated organic compounds that degrade in the presence of a hydroxyl radical, which substantially reduces the atmospheric lifetime.[5] HFOs have extremely low GWPs and zero ODP[6,7] making them excellent candidates to replace HFCs. In some applications, HFOs cannot be used in existing equipment as "drop-in" replacements for HFCs; therefore, blending HFOs with low-GWP HFCs and utilizing a mixture with tailored properties provides a suitable alternative for maintaining the life expectancy of the equipment.[8,9] HFC/HFO blends offer an optimal solution for current equipment; however, at the end of the equipment lifecycle, the HFC will likely have to be separated from the HFO in order to reblend the product or remove the HFC from service when new refrigeration systems are based on only HFO only refrigerants. For example, in the U.S., the EPA banned the use of HFC-134a (1,1,1,2-tetrafluoroethane, CH_2FCF_3) in 2021 for the manufacture of light-duty vehicles.[10] In the transitioning phase to HFO-based refrigerants, HFCs will be repurposed to create

Received: September 13, 2023
Revised: October 18, 2023
Accepted: October 19, 2023
Published: November 2, 2023

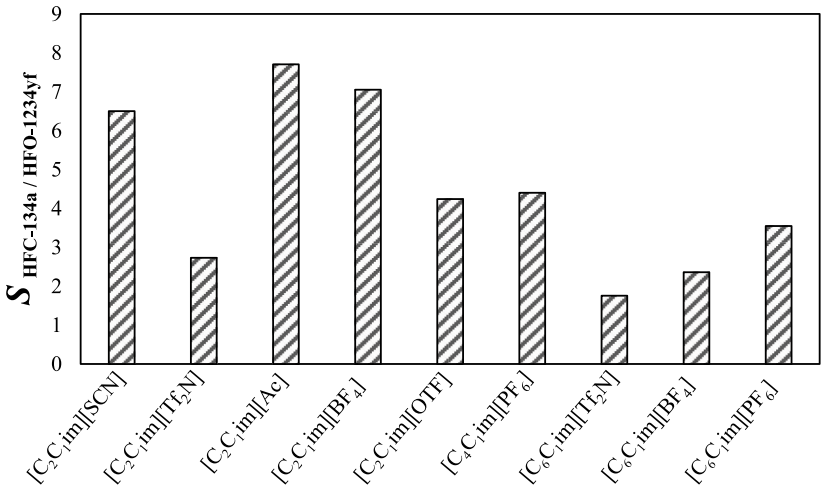

Figure 1. Selectivity of HFC-134a/HFO-1234yf in the ILs used in this work at 303.15 K and 0.5 MPa.

other chemicals or materials (e.g., conversion into vinylidene fluoride for polymer manufacturing)[11] or destroyed by incineration while HFOs will be recycled and reused. At the present time, HFCs are recycled with high purity to remove common impurities such as air, water, oil, and refrigerants that do not form azeotropes, so that the HFCs can reenter the market. However, if an azeotrope exists between one or more refrigerants, the current technology using fractional distillation is unable to separate the mixture. This issue will only increase and become more challenging as additional HFO refrigerants and mixtures enter the market, many of which form azeotropes with a number of existing refrigerants. Project EARTH (Environmentally Applied Research Toward Hydrofluorocarbons), a multiuniversity program led by the University of Kansas in collaboration with Notre Dame University and Rutgers University, is developing three technologies for the separation of HFC and HFC/HFO mixtures so that low GWP components can be recycled and high GWP components can be repurposed into environmentally safe products. These technologies are membrane separation, porous media separation, and extractive distillation with ionic liquid (IL) entrainers. The separation technologies overcome the challenges of azeotropic mixtures that are not possible to separate using fractional distillation. In this work, extractive distillation with ILs is simulated to separate the HFC/HFO mixture. This technology has been efficient in separating azeotropic and near-azeotropic HFC mixtures into high purity components.[12,13] Ionic liquids are molten salts at room temperature and are defined as having melting points below 373 K. ILs have negligible vapor pressure at room temperature and high thermal and chemical stability, which makes them ideal solvents for the extraction process rather than traditional organic solvents.[14] For a highly efficient HFC/HFC or HFC/HFO mixture separation with minimal work, the IL must be properly chosen based on the solubility and selectivity of the IL to one or more components of the mixture to allow the less soluble component to be extracted. Since ILs have negligible vapor pressure, using a pressure vacuum vessel or flash drum will extract the solute from the IL and assist with the recycle of the pure IL. In this study, R-513A is an azeotropic HFC/HFO mixture that consists of 44 wt % 1,1,1,2-tetrafluoroethane (HFC-134a) and 56 wt % 2,3,3,3-tetrafluoropropene (HFO-1234yf) and is a replacement for HFC-134a (GWP_{100} = 1300) with a 56% reduction in GWP (GWP_{100} = 573) and has similar energy efficiency.[15,16] The HFO-1234yf can be a substituent for HFC-134a, and it is compatible with many HFC-134a systems, but it is mildly flammable (A2L classification by ASHRAE), which can require additional safe guards, such as leak detectors, be put in place. In contrast, R-513A is a nonflammable refrigerant[17,18] and some existing systems that use HFC-134a may not be designed to use a mildly flammable refrigerant (e.g., HFO-1234yf). Kamiaka et al. found that mixing HFC-134a with HFO-1234yf terminates the mild flammability of HFO-1234yf and forms an azeotrope at 50/50 wt %.[16] R-513A is a nonflammable refrigerant mixture (A1, ASHRAE classification) composed of 44 wt % HFC-134a and 56 wt % HFO-1234yf and provides thermophysical properties similar to HFC-134a, which makes it a suitable alternative to HFC-134a in existing equipment.[19]

2. METHODOLOGY

Using extractive distillation with an IL as an entrainer has been demonstrated using ASPEN modeling. In order to minimize the required energy and maximize the efficiency of the separation, it is essential to accurately select the appropriate IL based on maximizing selectivity and solubility of the refrigerant in the IL. Experimental work and simulations appear promising for highly effective separation design to selectively recover high-purity refrigerants and recycle the IL.[12,13,20] This work is a simulation based on equilibrium modeling to provide the possibility of recovering the components of azeotropic mixture R-513A and recycling the IL entrainer to be continuously reused. Before the simulation, the equilibrium data of a chosen solvent and solute are regressed and fit with a thermodynamic model to predict the binary interaction parameters between solvent (i.e., IL) and solute (i.e., refrigerants). This requires the estimation of physical and critical properties of the components and ideal gas heat capacity using the group contribution theory for ILs. Achieving a low average absolute deviation (AAD) between predicted and experimentally measured properties provides confidence in the separation simulations. Operating conditions were optimized to find the overall best process design for achieving a refrigerant purity of at least 99.5 wt % that is required for meeting the AHRI 700 refrigerant purity standard.[21]

2.1. Ionic Liquid Screening. ILs have the advantage of tunability of the cations and anions to desired physical and chemical properties that meet the requirements for the specific

https://doi.org/10.1021/acs.iecr.3c03245
Ind. Eng. Chem. Res. 2023, 62, 19862−19872

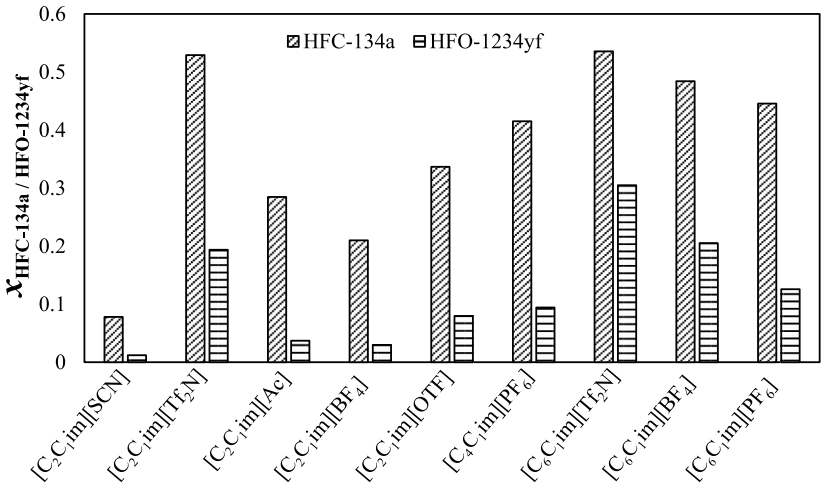

Figure 2. Solubility of HFC-134a/HFO-1234yf in ILs used in this work at 303.15 K and 0.5 MPa.

application.[14] Among the thousands of ILs that can be synthesized, the selectivity and solubility differences of the mixture components in the IL aid the user in designing the best separation process. Solubility measurements (e.g., vapor−liquid equilibrium, VLE) help narrow the choice for a suitable IL to achieve the required separation of interest. In this study, solubility data of HFC-134a and HFO-1234yf were found for nine different imidazolium-based ILs. The advantages of imidazolium-based ILs are high-temperature stability and broad liquidus range,[22] which will maximize the potential for being solvents (i.e., entrainers) in extractive distillation. The ILs chosen for this study with large differences in HFC-134a/HFO-1234yf solubility include 1-ethyl-3-methylimidazolium acetate $[C_2C_1im][Ac]$, 1-ethyl-3-methylimidazolium tetrafluoroborate $[C_2C_1im][BF_4]$, 1-ethyl-3-methylimidazolium trifluoromethanesulfonate $[C_2C_1im][OTF]$, 1-ethyl-3-methyl-imidazolium thiocyanate $[C_2C_1im][SCN]$, 1-ethyl-3-methylimidazolium bis(trifluoromethylsulfonyl)imide $[C_2C_1im][Tf_2N]$, 1-butyl-3-methylimidazolium hexafluorophosphate $[C_4C_1im][PF_6]$, 1-hexyl-3-methylimidazolium tetrafluoroborate $[C_6C_1im][BF_4]$, 1-hexyl-3-methylimidazolium hexafluorophosphate $[C_6C_1im][PF_6]$, and 1-hexyl-3-methylimidazolium bis(trifluoromethylsulfonyl)imide $[C_6C_1im][Tf_2N]$ as shown in Figure 1. Based on the high selectivity and solubility differences published in literature,[24−43] these ILs were chosen to model as entrainers for the separation of R-513A using extractive distillation. The possible reasons for the solubility differences are diversity in molecular weight, cation alkyl chain length, and possibilities for hydrogen bonding or other physical interactions (e.g., dispersion forces). The solubility for both HFC-134a and HFO-1234yf increased in the ILs with the higher molecular weight.[23] In addition, the solubility increases with longer alkyl chain for the cation of the IL,[23,24] as shown in Figure 2 with the same anions (e.g., $[Tf_2N]$, $[BF_4]$, and $[PF_6]$). The solubility of HFC-134a and HFO-1234yf is higher with ILs that have a greater possibility for hydrogen bonding.[25] For example, the $[Tf_2N]$ anion can form hydrogen bonds with HFC-134a and HFO-1234yf due to the presence of sulfonyl groups and fluorine atoms, and the solubility of the refrigerants was higher in ILs with the $[Tf_2N]$ anion.

The selectivity was defined as the ratio of pure gas solubilities in the liquid phase at a given temperature and pressure, as shown in eq 1

$$S_{j/i}(T, P) = \left(\frac{X_j}{X_i}\right) \tag{1}$$

where i and j are mole fractions of gas i and gas j dissolved in the IL.

Another important factor, particularly for the economic feasibility, is the solubility of the refrigerant in the IL. To illustrate, for a given azeotropic binary mixture, if the selectivity is high but the solubility of both refrigerants is low, a large flow rate of solvent is needed to separate the azeotropic mixture. Figure 2 shows the solubility of HFC-134a and HFO-1234yf in ILs.

A high solubility difference of HFO-1234yf and HFC-134a was found in $[C_2C_1im][SCN]$, which results in a high selectivity, but both refrigerants have low solubility, and this IL would not be a good choice for the separation of R-513A. The $[C_2C_1im][Ac]$ has the highest selectivity among the nine ILs considered with a moderate solubility for HFC-134a and low solubility of HFO-1234yf making it a better choice than $[C_2C_1im][SCN]$.

2.2. Thermodynamic Model. The Peng−Robinson EOS with Boston−Mathias and standard mixing rule (PR-BM)[26,27] was used to model the vapor−liquid equilibrium (VLE) and liquid−liquid equilibrium (LLE) data. PR-BM describes the binary interaction between a refrigerant and the IL, which helps to estimate other mixture properties that will be needed for the simulation.

The PR EOS with BM and standard mixing rule is

$$P = \frac{RT}{V_m - b} - \frac{a}{V_m(V_m + b) + b(V_m - b)} \tag{2}$$

where

$$b = \sum_i x_i b_i \tag{3}$$

$$a = a_0 + a_1 \tag{4}$$

$$a_0 = \sum_i \sum_j x_i x_j (a_i a_j)^{0.5}(1 - k_{ij}) \tag{5}$$

https://doi.org/10.1021/acs.iecr.3c03245
Ind. Eng. Chem. Res. 2023, 62, 19862−19872

Table 1. Binary Interactions with Average Absolute Deviation (AAD)[a]

(*i*)	(*j*)	$N_{Experiments}$	$N_{Temperature}$	temperature range [K]	$k_{ij}(1)$	$k_{ij}(2)$	$l_{ij}(1)$	$l_{ij}(2)$	average absolute deviation			references
									T (K)	P (MPa)	x_i (%)	
HFC-134a	$[C_2C_1im][SCN]$	20	4	283.15−313.15	−0.1619	0.0010	−0.0142	−0.0005	0.1115	0.0008	0.144	24
HFO-1234yf		20	4	283.15−313.15	−1.1774	0.0052	0.1339		3.3268	0.0090	0.005	24
HFC-134a	$[C_2C_1im][TF_2N]$	46	5	283.15−348.1	0.0036	−0.0004	−0.0090	0.00011	0.1557	0.0702	0.00076	34
LLE		4	4	333.15−349.1					4.6251	5.0124	2.672	34
HFO-1234yf		50	5	283.15−323.15	−0.1123	0.0005	−0.1693	0.00057	0.4592	0.0041	0.00014	35
HFC-134a	$[C_2C_1im][Ac]$	13	1	303.15	0.0103		−0.1067		0.0780	0.0005	0.256	36
HFO-1234yf		49	7	283.15−343.15	−0.2586	0.0015	−0.2042	0.0009	0.0109	0.1055	0.001	37
HFC-134a	$[C_2C_1im][BF_4]$	36	5	283.15−323.15	−0.2771	0.0013	−0.1620	0.0004	0.0890	0.0007	0.251	35
HFO-1234yf		54	7	283.15−343.15	0.8635	−0.0021	2.3546	−0.0081	0.0493	0.0005	0.026	38
HFC-134a	$[C_2C_1im][OTF]$	31	5	283.15−323.15	−0.1250	0.0005	−0.0640	0.0002	0.0435	0.0003	0.199	35
HFO-1234yf		25	5	283.15−323.15	−0.1991	0.0010	0.3074	−0.0010	0.2105	0.0015	0.222	35
HFC-134a	$[C_4C_1im][PF_6]$	31	4	283−348.2	−0.2237	0.00084	−0.7527	0.0019	0.0153	0.0789	0.4	39
LLE		3	3	318.2−355					0.00006	6.307	2.14	40
HFO-1234yf		49	7	283.15−343.15	−0.0247	0.0007	0.1159	−0.0005	0.0000	0.0000	0.046	41
HFC-134a	$[C_6C_1im][TF_2N]$	39	3	298.15−348.15	0.2262	−0.0008	−0.1977	0.0006	0.3801	0.1357	0.064	42
HFO-1234yf		39	7	293.15−353.15	0.0638	−0.0001	0.0604	−0.0003	0.0000	0.0108	0.042	43
HFC-134a	$[C_6C_1im][BF_4]$	16	3	298−348	−0.2611	0.0010	0.8122	*−0.0028*	0.0001	0.2920	0.113	42
HFO-1234yf		54	7	283.15−343.15	0.0654	0.0002	0.3973	−0.0015	0.0000	0.0159	0.046	38
HFC-134a	$[C_6C_1im][PF_6]$	21	3	298−348	0.0043	0.0001	−0.2454	0.0005	0.0000	0.1130	0.009	42
HFO-1234yf		49	7	283.15−343.15	0.0057	0.0006	0.1040	−0.0003	0.0002	0.0027	0.057	41

[a] $N_{Experiments}$ = number of experimental data point, $N_{Temperature}$ = number of temperatures that measurement conducted at.

https://doi.org/10.1021/acs.iecr.3c03245
Ind. Eng. Chem. Res. 2023, 62, 19862−19872

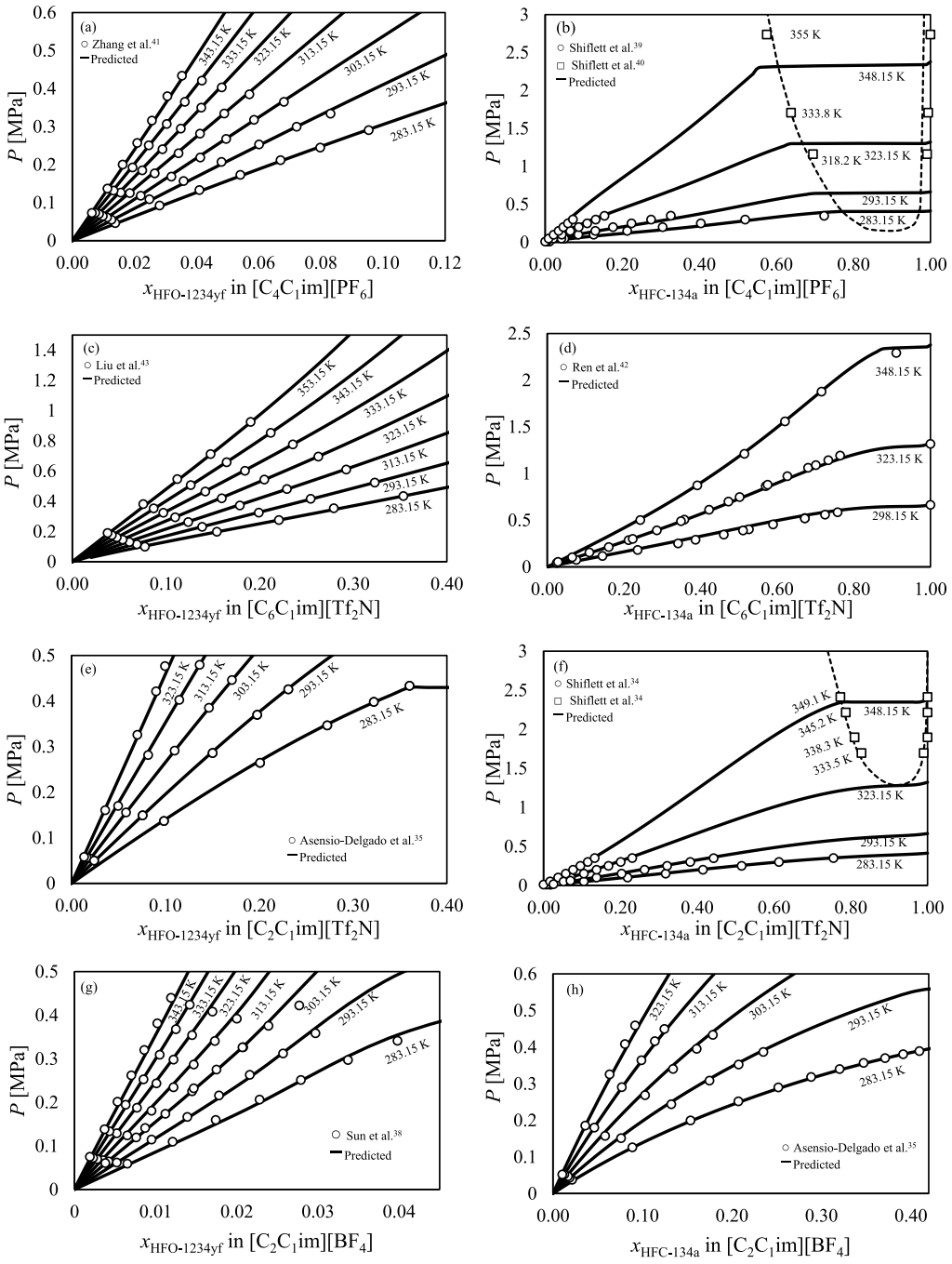

Figure 3. *PTx* diagrams for HFO-1234yf and HFC-134a in ILs (*PTx* diagrams for the other ILs are in the Supporting Information).

$$k_{ij} = k_{ij}^{(1)} + k_{ij}^{(2)}T + \frac{k_{ij}^{(3)}}{T}$$
$$k_{ij} = k_{ji} \tag{6}$$

$$a_1 = \sum_{i=1}^{n} x_i \left(\sum_{j=1}^{n} x_j ((a_i a_j)^{1/2} l_{ij})^{1/3} \right)^3 \tag{7}$$

$$l_{ij} = l_{ij}^{(1)} + l_{ij}^{(2)}T + \frac{l_{ij}^{(3)}}{T}$$
$$l_{ij} \neq l_{ji} \tag{8}$$

The parameters, a and b, are a function of the pure component critical properties (T_c, P_c, ω). The mixing terms (k_{ij} and l_{ij}) are the binary interaction parameters that are determined by the regression of the equilibrium data. Fitting these parameters to VLE data allows using a PR-BM thermodynamic model that describes the behavior of the system. For process design, optimization, and simulation, an accurate descriptive behavior of the VLE system is needed. The accurate descriptive behavior of the system is based upon the accuracy of estimating these parameters, which can be determined by a lower AAD % and the agreement between estimated and experimental *PTx* diagrams as shown in Table 1 and Figure 3.

https://doi.org/10.1021/acs.iecr.3c03245
Ind. Eng. Chem. Res. 2023, 62, 19862−19872

Table 2. Physical and Critical Properties for ILs and Refrigerants Used in This Work[28,29]

name	formula	MW (g mol^{-1})	T_b (K)	T_c (K)	P_c (MPa)	V_c (cm^3 mol^{-1})	Z_c	Ω
$[C_2C_1im][Ac]$	$C_8H_{14}N_2O_2$	170.2	*578.8*	*807.1*	*2.29*	*544*	0.2367	0.5889
$[C_2C_1im][BF_4]$	$C_6H_{11}N_2BF_4$	197.97	*449.5*	*1234.4*	*2.36*	*540*	0.2573	0.8087
$[C_2C_1im][OTF]$	$C_7H_{11}F_3N_2O_3S$	260.23	*662*	*992.3*	*3.58*	*636.4*	0.2765	0.3255
$[C_2C_1im][SCN]$	$C_7H_{11}N_3S$	169.3	*717.3*	*1013.6*	*2.23*	*666.4*	0.176	0.3931
$[C_2C_1im][Tf_2N]$	$C_8H_{11}N_3F_6S_2O_4$	391.3	816.7	1249.3	3.27	875.9	0.2753	0.2157
$[C_4C_1im][PF_6]$	$C_8H_{15}N_2PF_6$	284.2	554.6	719.4	1.73	762.5	0.2203	0.7917
$[C_6C_1im][BF_4]$	$C_{10}H_{19}BF_4N_2$	254.08	541	1080.6	1.79	769.2	0.2406	0.9625
$[C_6C_1im][PF_6]$	$C_{10}H_{19}F_6N_2P$	312.24	600.3	764.9	1.55	876.7	0.2137	0.8697
$[C_6C_1im][Tf_2N]$	$C_{12}H_{19}N_3F_6S_2O_4$	447.41	908.2	1292.8	2.39	1104.4	0.2454	0.3893
HFC-134a	$C_2H_2F_4$	102.03	247.08	374.18	4.057	0.2002	0.26103	0.32695
HFO-1234yf	$C_3H_2F_4$	114.04	243.65	367.85	3.379	0.2403	0.32695	0.2753

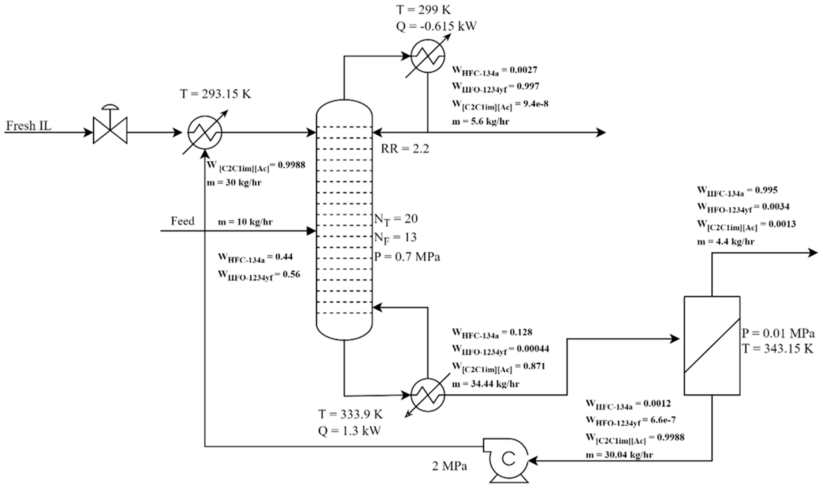

Figure 4. Process flow diagram for R-513A separation using the $[C_2C_1im][Ac]$ IL. PFDs using other ILs are provided in the Supporting Information.

The experimental *PTx* data for HFC-134a and HFO-1234yf in ILs were fit with the PR-BM model to minimize the error to be less than 10% AAD. The smaller the % AAD, the more accurate the simulation. Using eqs 6, 7, and 8, and setting $k_{ij} = k_{ji}$ and $l_{ij} \neq l_{ji}$, the PR-BM has nine parameters to fit the binary interactions (i.e., refrigerant + IL). In this work, l_{ij} was assumed to be equal to l_{ji} ($l_{ij} = l_{ji}$) and $k_{ij}^{(3)}$ and $l_{ij}^{(3)}$ were fixed, reducing the number of parameters to four parameters instead of nine, as shown in Table 1. The predictions fit the experimental data with a low % AAD. The binary interactions of HFC-134a and HFO-1234yf in ILs with the % AAD are shown in Table 1. The critical properties of ILs were obtained from Valderrama and Rojas; however, for ILs like $[C_2C_1im][BF_4]$, the critical temperature (T_c) was obtained from a different source (Sattari et al.), which estimated the critical temperature using the Guggenheim model, group contribution (GC), and quantitative structure−property relationship (QSPR). These three models are in good agreement and deviate from Valderrama and Rojas, which estimates the critical temperature using the "modified Lydersen−Joback−Reid" method.[28,29] Valderrama and Rojas has been widely used in different applications. (e.g., Gardas et al.[30] has used Valderrama and Rojas critical properties for estimating density of five ILs and the estimations were in good agreement with the experimental measurements). However, Sattari et al. have found a high deviation in T_c calculation especially for ILs with the tetrafluoroborate $[BF_4]$ anion. Moreover, T_c of Valderrama and Rojas in the ASPEN Plus simulator overestimates the vapor pressure of $[C_2C_1im][BF_4]$, which was 385 Pa at 323.15 K. This vapor pressure is significantly high in comparison to $[C_2C_1im][SCN]$, $[C_2C_1im][Ac]$, and $[C_2C_1im][OTF]$ which are 0.173, 0.02, and 1.34 Pa, respectively, at the same temperature. The high vapor pressure estimation of ILs complicates the separation in the flash because if the flash operates at a low vacuum of 0.05 MPa, the gas extraction from IL may not be maximized. As a result, there will be some amount of refrigerant contaminated with the IL, reducing the overall refrigerant purity. On the other hand, if the flash operates at a high vacuum of 0.01 MPa, the IL with a high vapor pressure will partially evaporate and contaminate the extracted refrigerant, reducing the purity. The estimated T_c = 596.2 K for $[C_2C_1im][BF_4]$ by Valderrama and Rojas complicates the separation process by overestimating the vapor pressure of the IL so that there is a trade-off between the purity of the refrigerant and the purity of the IL. The estimated T_c of Sattari et al. using QSPR for $[C_2C_1im][Tf_2N]$ is 1209.7 K. A similar value for the T_c was estimated using the EÖtvos equation by Rebelo et al.[31] The T_c reported by Valderrama and Rojas was 1249.3 K. For $[C_2C_1im][Tf_2N]$, the difference in T_c reported is small, but for other ILs, there can be a larger difference. Vapor pressure of $[C_2C_1im][Tf_2N]$ using T_c = 1209.7 K (estimated by QSPR and EÖtvos equation) is 9.6 × 10^{-7} Pa at 358.15 K, which is relatively close to the measured vapor pressure by Ahrenberg et al. using a highly sensitive method for mass loss and the Langmuir equation to calculate a vapor pressure of 1.3 × 10^{-6} Pa at the same temperature (358.15 K).[32] The T_c for some ILs were estimated using QSPR

https://doi.org/10.1021/acs.iecr.3c03245
Ind. Eng. Chem. Res. 2023, 62, 19862−19872

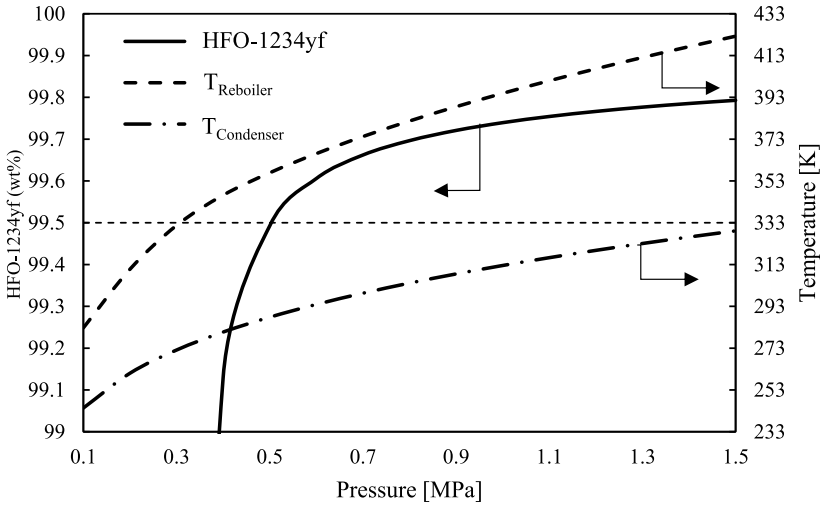

Figure 5. HFO-1234yf purity, reboiler T, and condenser T as a function of pressure using IL $[C_2C_1im][Tf_2N]$.

reported by Sattari et al. Table 2 summarized the physical and critical properties of ILs and refrigerants, which were used in the Aspen modeling. The ideal gas heat capacity for all ILs was estimated by using the extended Joback method with group contribution parameters proposed by Ge et al.[33] The regressed ideal gas heat capacity of ILs is provided in the Supporting Information.

3. SIMULATION

ASPEN Plus was used to simulate the separation of R-513A with an equilibrium-based extractive distillation model. The process consisted of a single extractive distillation column with a reboiler and condenser for separation of the light component, followed by a flash vessel to recycle the IL and separate the heavy component. For the separation of R-513A, HFO-1234yf is less soluble in the ILs and was the distillate product (i.e., light component). The HFC-134a is more soluble in the ILs and was the bottom product (i.e., heavy component). The IL + HFC-134a was separated in the flash tank, and the IL recycled. A process flow diagram is shown in Figure 4 with typical operating conditions for IL $[C_2C_1im][Ac]$.

4. OPTIMIZATIONS

The process design is based on a pilot-scale extractive distillation column operating in a high-bay area at the University of Kansas (KU). Operational constraints, such as the maximum $T_{Reboiler}$ and minimum $T_{Condenser}$, have been described in previous work by Finberg et al.,[12] and the ideal case is to have $T_{Reboiler} < 373.15$ K and $T_{Condenser} > 293.15$ K. The decomposition temperature (T_{onset}) for the studied ILs ranges from about 494.15 to 703.15 K. T_{onset} for $[C_2C_1im][Ac]$ is the lowest which is 494.15 K and was found to start decomposition at 413 K.[44] To prevent any decomposition of the IL, the maximum $T_{Reboiler} < 403.15$ K. The building chilled water supply can maintain a condensing temperature of about 298.15 K. The $T_{Reboiler}$ and $T_{Condenser}$ can be adjusted by changing the column pressure and solvent-to-feed (S/F) ratio to achieve the highest product purities with the lowest energy consumption. The feed stage (N_F) can be optimized after setting the S/F ratio, pressure, and number of theoretical stages (N_T). The reflux ratio (RR) can be adjusted for optimal distillate purity (i.e., HFO-1234yf). If purity cannot be achieved by optimizing these parameters, then increasing the number of stages can improve the overall separation performance. If the desired purity could not be achieved, then a different IL was considered. This methodology was used for optimizing the process simulation for the separation of R-513A with nine ILs.

4.1. Sensitivity Analysis. A sensitivity analysis was performed to assess the effect of changes to several variables on product purity and total energy consumption, which included pressure, S/F ratio, N_F, N_T, RR, heat duty of the condenser and/or reboiler, and temperature of the condenser and reboiler. Upper limits for some variables were specified such as $N_T \leq 40$, S/F ratio $\leq 10/1$, $T_{Reboiler} < 403.15$ K, and $T_{Condenser} > 298.15$ K. The purity target was a minimum of 99.5 wt % for both HFO-1234yf and HFC-134a.

A feed flow rate of 10 kg/h for R-513A was selected for all simulations based on the size of the extractive distillation column at KU, and the entrainer (i.e., IL) was fed to the top of the column on solvent stage ($N_S = 2$).[45] For complete separation, the distillate rate should be equal to the mass fraction of the light key component (i.e., HFO-1234yf) multiplied by the feed flow rate.[13] For example, R-513A is composed of 56 wt % HFO-1234yf and 44 wt % HFC-134a, and the distillate rate is equal to about 5.6 kg/h with a feed flow rate of 10 kg/h. The sensitivity of each parameter was evaluated in the following order: S/F → P → N_T → N_F → RR, which was developed by Finberg and Shiflett.[13]

4.1.1. S/F Ratio. The S/F ratio is dependent on the solubility and selectivity of the refrigerants in the IL and the desired product purity required for the separation. A sensitivity analysis begins with the S/F ratio for achieving the highest product purity. The solubility and selectivity at a given T and P can provide some insight into the suitability of the IL for the desired separation. For example, in the case of IL $[C_2C_1im][SCN]$, $x_{HFC\text{-}134a} = 0.078$ and $x_{HFO\text{-}1234yf} = 0.012$ at $T = 303.15$ K and $P = 0.5$ MPa. The low solubilities for both refrigerants resulted in a higher S/F ratio. The high selectivity of about 6.5 resulted in a higher product purity. The ideal scenario is for one refrigerant to have a high solubility and the other refrigerant to have a low solubility. Among the nine ILs investigated in this study, $[C_2C_1im][Ac]$ has the highest selectivity with moderate solubility for HFC-134a and low solubility for HFO-1234yf, which resulted in the lowest S/F ratio for this IL, see Supporting Information.

https://doi.org/10.1021/acs.iecr.3c03245
Ind. Eng. Chem. Res. 2023, 62, 19862−19872

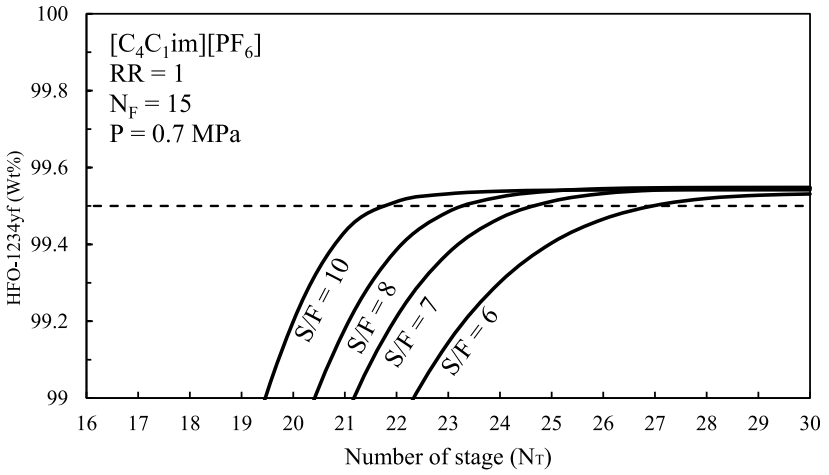

Figure 6. HFO-1234yf purity as a function of the S/F ratio and number of stages for $[C_4C_1im][PF_6]$.

4.1.2. Pressure. The HFO-1234yf product purity is highly affected by the column pressure, as shown in Figure 5. The higher the column pressure, the higher the refrigerant solubility in the IL, as shown in Figure 3a–h. However, higher pressure increases the reboiler temperature, and ideally the $T_{Reboiler}$ < 403.15 K to avoid IL decomposition. In addition, lower pressure decreases the condensing temperature and, ideally, the $T_{Condenser}$ > 298.15 K so that chilled water can be utilized versus refrigeration. Therefore, choosing the desired HFO-1234yf product purity will determine the operating P, $T_{Reboiler}$, and $T_{Condenser}$ values, as shown in Figure 5.

4.1.3. Number of Stages (N_T). The number of stages (N_T) is influenced by several factors, such as feed composition, product purity, operating T and P, diameter of the distillation column, and S/F ratio. Feed composition in this case is fixed, which is 44 wt % HFC-134a and 56 wt %% HFO-1234yf. A lower S/F ratio required a higher number of stages to achieve the same product purity, which meant a taller distillation column. In contrast, a higher S/F ratio may allow for a shorter distillation column, but the diameter would have to increase to handle the higher IL flow rate and vice versa. In this report, the number of stages (N_T) were calculated to achieve a product purity for HFO-1234yf (≥99.5 wt %) and HFC-134a (≥99.5 wt %). The diameter of the column was not calculated by using the equilibrium-based model. Using IL $[C_4C_1im][PF_6]$, the HFO-1234yf purity was achieved with either S/F = 10 and N_T = 18 stages or S/F = 5 and N_T = 25 stages, as shown in Figure 6. If the extractive distillation column already exists with a specific number of stages so that N_T cannot be changed, then the S/F ratio, P, and RR can be optimized for obtaining the desired purity. In addition to a lower S/F ratio with a higher number of stages, Lek-utaiwan et al.[46] found that increasing the number of stages reduces the energy consumption due to a decrease in the reboiler and condenser duties, which reduces the operating costs.

4.1.4. Feed Stage (N_F). The effect of feed stage location and reboiler T and P on HFO-1234yf purity is shown in Figure 7. An optimal N_F for the separation of R-513A using IL $[C_2C_1im][Tf_2N]$ is between stages 11 to 13 based on what reboiler temperature is chosen.

4.1.5. Reflux Ratio (RR). A higher reflux ratio (RR = 1 to 4) increased the HFO-1234yf purity, but had an overall small effect (99.6 to 99.7 wt %) with IL $[C_4C_1im][PF_6]$ compared with other variables (e.g., S/F, P, N_T, and N_F), as shown in Figure 8. A higher RR also decreased the distillation column temperature and required higher energy input for the reboiler, therefore, increasing the operating costs.[45,47]

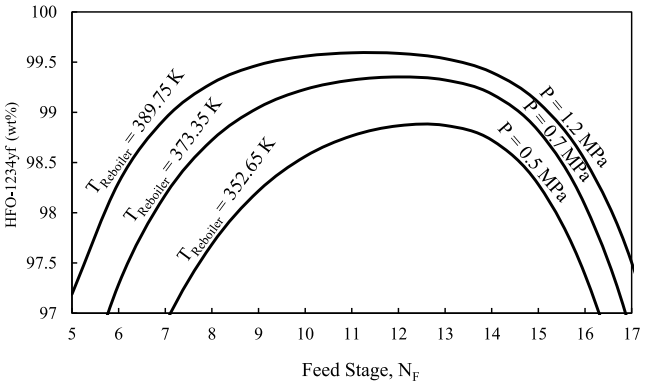

Figure 7. HFO-1234yf purity as a function of the feed stage, reboiler temperature, and pressure for fixed N_T = 23 using IL $[C_2C_1im][Tf_2N]$.

4.1.6. Flash Tank Temperature and Pressure. The purity of HFC-134a recovered from the flash tank was calculated over specific ranges of T and P to obtain the desired purity, as shown in Figure 9. A minimum of T = 365 K and P = 0.01 MPa was required in order to achieve the desired HFC-134a purity of 99.5 wt % with $[C_2C_1im][Tf_2N]$.

5. RESULTS AND DISCUSSION

In this work, nine ILs were modeled using ASPEN Plus to simulate the separation process of the azeotropic mixture R-513A. The process for each IL was optimized to achieve ≥99.5 wt % HFO-1234yf and ≥99.5 wt % HFC-134a with the operating conditions and heat duties provided in Table 3.

The IL $[C_2C_1im][Ac]$ demonstrated the lowest S/F ratio value of 3. $[C_2C_1im][SCN]$, $[C_2C_1im][BF_4]$, $[C_2C_1im][Ac]$, and $[C_2C_1im][OTF]$ exhibited the least number of stages (N_T = 19 to 21). In addition, $[C_6C_1im][Tf_2N]$ had the largest RR = 4. The IL with the lowest operating pressure (P = 0.5 MPa) was $[C_6C_1im][BF_4]$. The ILs with the lowest reboiler temperatures ($T_{Reboiler}$ = 319.8 to 334.5 K) were $[C_2C_1im][Ac]$, $[C_2C_1im][OTF]$, and $[C_6C_1im][BF_4]$. The IL with the

https://doi.org/10.1021/acs.iecr.3c03245
Ind. Eng. Chem. Res. 2023, 62, 19862−19872

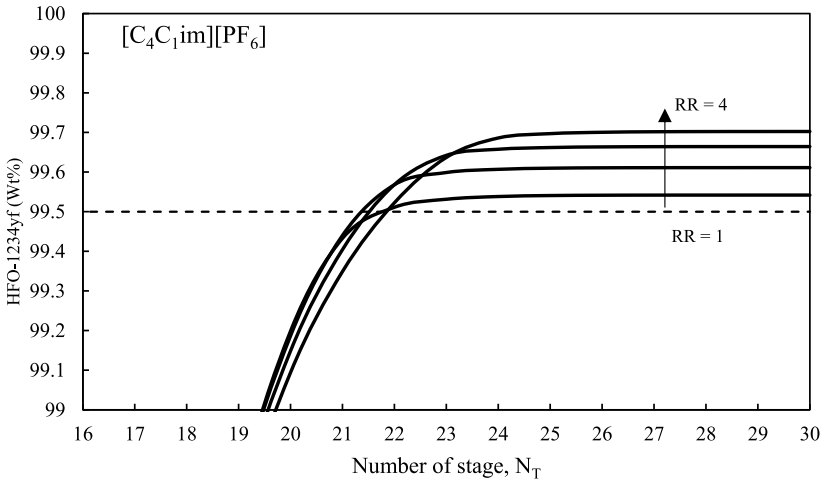

Figure 8. HFO-1234yf purity as a function of the number of stages and reflux ratio for IL $[C_4C_1im][PF_6]$ with S/F = 10, P = 0.7 MPa, and N_F = 15.

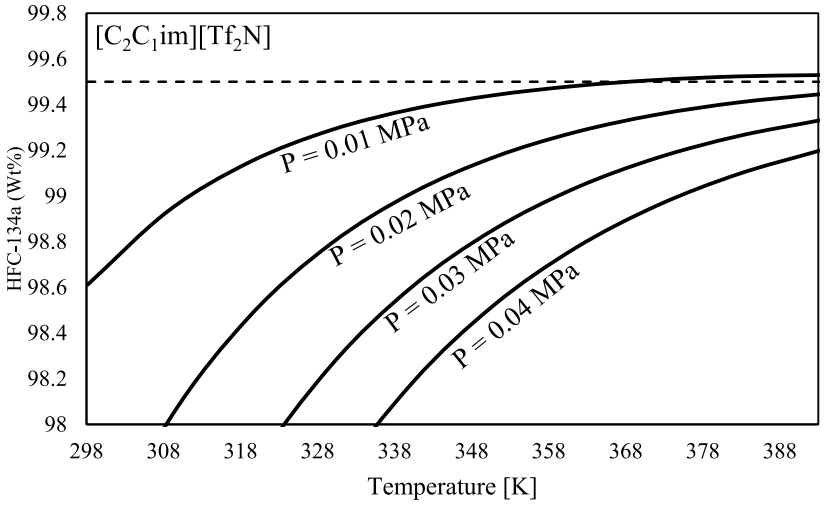

Figure 9. HFC-134a purity as a function of T and P in a flash tank.

Table 3. Summary of the Operating Conditions and Heat Duties for the ILs Used in This Simulation

ionic liquid	solvent-to-feed ratio	number of stages	feed stage	reflux ratio	pressure	reboiler temperature [K]	condenser temperature [K]	condenser heat duty [kW]	reboiler heat duty [kW]	flash tank net duty [kW]	cooler heat duty [kW]	overall absolute energy demand [kW]
$[C_2C_1im][Ac]$	3	20	13	2.2	0.7	333.91	299.04	−0.62	1.3	0.39	−0.823	3.133
$[C_2C_1im][BF_4]$	4.7	20	12	3	0.6	340.51	293.65	−0.88	2.92	−0.31	−1.62	5.73
$[C_2C_1im][SCN]$	11.2	19	12	2	1.2	346.44	319.78	−0.46	2.83	1.13	−3.47	7.89
$[C_2C_1im][Tf_2N]$	5.6	23	13	2	1.4	386	326.17	−0.49	2.54	0.38	−2.01	5.42
$[C_2C_1im][OTF]$	5.2	21	13	2	0.7	334.5	299.04	−0.64	1.65	0.53	−1.31	4.13
$[C_4C_1im][PF_6]$	5.7	24	12	2.1	0.7	347.8	299.29	−0.66	1.75	−0.29	−0.6	3.3
$[C_6C_1im][PF_6]$	5.7	26	17	2	0.8	364.2	304.11	−0.62	2.4	−0.61	−0.97	4.6
$[C_6C_1im][Tf_2N]$	6	39	21	4	1	397.19	312.55	−0.99	4.06	−1.41	−1.41	7.87
$[C_6C_1im][BF_4]$	6	36	21	2	0.5	319.8	287.66	−0.71	1.33	0.54	−1.03	3.61

highest condensing temperature ($T_{Condenser}$ = 326 K) was $[C_2C_1im][Tf_2N]$. Perhaps the most important ILs are those with the lowest overall absolute energy demand. For example, $[C_2C_1im][Ac]$ has a condenser duty of −0.62 kW, a reboiler duty of 1.3 kW, a flash tank net duty of 0.39 kW, and a cooler duty of −0.82 kW for a total of 3.13 kW, the lowest among the

https://doi.org/10.1021/acs.iecr.3c03245
Ind. Eng. Chem. Res. 2023, 62, 19862−19872

nine ILs studied. The simulations were based on equilibrium, so results could be different using a rate-based model that takes into account transport properties. For example, ILs tend to be more viscous than ordinary solvents and could affect the rate of mass transport. However, the viscosity of the IL is significantly reduced by the solubility of the refrigerant dissolved in the liquid as described by Ahosseini et al.[48] and other groups.[49,50] In addition, Viar et al.[51] conducted a similar separation process using rate-based and equilibrium models to separate R-410A using three different ILs with low, moderate, and high viscosities and demonstrated the significance of mass transport properties in the design of extractive distillation. Future work will test these ILs in a pilot-scale extractive distillation to validate the modeling results, and ASPEN Plus rate-based models are under development.

6. CONCLUSIONS

Extractive distillation using IL entrainers has been shown to be effective at separating azeotropic refrigerant mixtures based on ASPEN Plus simulations supported with global phase behavior data. This report demonstrates the process for separating R-513A into HFO-1234yf and HFC-134a with a purity of ≥99.5 wt % and recycling the IL. When utilizing ionic liquids (ILs) as entrainers for the separation of R-513A, the operational conditions and total heat duty can experience a more than 2-fold increase. Among various ILs studied, $[C_2C_1im][Ac]$ demonstrated the potential to achieve minimal operating conditions (i.e., low solvent/feed ratio, number of theoretical stages, and reflux ratio) and heat duty. Conversely, when $[C_6C_1im][Tf_2N]$ was used instead of $[C_2C_1im][Ac]$, more than twice the overall energy was required for the separation of R-513A. Moreover, $[C_6C_1im][Tf_2N]$ required twice the amount of solvent and the number of stages increased relative to $[C_2C_1im][Ac]$. Thus, the selection of the appropriate ILs is crucial for optimizing the overall energy consumption (i.e., variable cost) and physical structure (i.e., capital cost) of the unit. This work demonstrated the variations in operating conditions and overall energy consumptions for heating and cooling duties resulting from the use of nine different ILs to separate R-513A. The results of the equilibrium-based simulation are promising; however, experimental work is still needed to validate the simulations.

■ ASSOCIATED CONTENT

Supporting Information

The Supporting Information is available free of charge at https://pubs.acs.org/doi/10.1021/acs.iecr.3c03245.

Additional ionic liquids properties, chemical structures, and abbreviations; vapor−liquid equilibria data and modeling; ideal gas heat capacity as a function of temperature for ILs; and ASPEN Plus process simulations (PDF)

■ AUTHOR INFORMATION

Corresponding Author

Mark B. Shiflett − *Institute for Sustainable Engineering, University of Kansas, Lawrence, Kansas 66045, United States; Department of Chemical and Petroleum Engineering, University of Kansas, Lawrence, Kansas 66045, United States;* orcid.org/0000-0002-8934-6192; Email: Mark.B.Shiflett@ku.edu

Author

Abdulrhman M. Arishi − *Institute for Sustainable Engineering, University of Kansas, Lawrence, Kansas 66045, United States; Department of Chemical and Petroleum Engineering, University of Kansas, Lawrence, Kansas 66045, United States; Department of Chemical Engineering, Jazan University, Jazan 82822, Saudi Arabia;* orcid.org/0009-0001-9482-0143

Complete contact information is available at: https://pubs.acs.org/10.1021/acs.iecr.3c03245

Notes

The authors declare no competing financial interest.

■ REFERENCES

(1) Duan, H. B.; Miller, T. R.; Liu, G.; Zeng, X. L.; Yu, K. L.; Huang, Q. F.; Zuo, J.; Qin, Y. F.; Li, J. H. Chilling Prospect: Climate Change Effects of Mismanaged Refrigerants in China. *Environ. Sci. Technol.* **2018**, *52* (11), 6350−6356.

(2) The Montreal Protocol on Substances That Deplete the Ozone Layer - United States Department of State. https://www.state.gov/key-topics-office-of-environmental-quality-and-transboundary-issues/the-montreal-protocol-on-substances-that-deplete-the-ozone-layer (accessed July 21, 2023).

(3) Schulz, M.; Kourkoulas, D. Regulation (EU) No 517/2014 of the European Parliament and of the Council of 16 April 2014 on Fluorinated Greenhouse Gases and Repealing Regulation (EC) No 842/2006. *Official Journal of the European Union* **2014**, L150.

(4) USEPA. *Proposed Rule—Phasedown of Hydrofluorocarbons: Establishing the Allowance Allocation and Trading Program under the AIM Act*; USEPA, 2021.

(5) Minjares, R. Refrigerants for light-duty passenger vehicle air conditioning systems. In *Proceedings of ICCT*, 2011.

(6) Booten, C.; Nicholson, S.; Mann, M.; Abdelaziz, O. *Refrigerants: Market Trends and Supply Chain Assessment*; Clean Energy Manufacturing Analysis Center, 2020.

(7) Sun, Y. J.; Wei, Q. M.; Wang, X. D.; Wang, X. P.; He, M. G. Absorption Separation of Hydrofluorocarbon/Hydrofluoroolefin Refrigerant Mixtures Using Ionic Liquids. *Ind. Eng. Chem. Res.* **2022**, *61* (34), 12787−12796.

(8) Kumar, A.; Chen, M.-R.; Hung, K.-S.; Liu, C.-C.; Wang, C.-C. A Comprehensive Review Regarding Condensation of Low-GWP Refrigerants for Some Major Alternatives of R-134a. *Processes* **2022**, *10* (9), 1882.

(9) Alam, M. S.; Jeong, J. H. Thermodynamic properties and critical parameters of HFO-1123 and its binary blends with HFC-32 and HFC-134a using molecular simulations. *Int. J. Refrig.* **2019**, *104*, 311−320.

(10) *Significant New Alternatives Policy. Environmental Protection Agency 40 CFR Part 82*, 2009.

(11) Han, W. F.; Kennedy, E. M.; Mackie, J. C.; Dlugogorski, B. Z. Conversion of a CFCs, HFCs and HCFCs waste mixture via reaction with methane. *J. Hazard. Mater.* **2010**, *184* (1−3), 696−703.

(12) Finberg, E. A.; May, T. L.; Shiflett, M. B. Multicomponent Refrigerant Separation Using Extractive Distillation with Ionic Liquids. *Ind. Eng. Chem. Res.* **2022**, *61* (27), 9795−9812.

(13) Finberg, E. A.; Shiflett, M. B. Process Designs for Separating R-410A, R-404A, and R-407C Using Extractive Distillation and Ionic Liquid Entrainers. *Ind. Eng. Chem. Res.* **2021**, *60* (44), 16054−16067.

(14) Pârvulescu, V. I.; Hardacre, C. Catalysis in ionic liquids. *Chem. Rev.* **2007**, *107* (6), 2615−2665.

(15) Mota-Babiloni, A.; Navarro-Esbrí, J.; Barragán-Cervera, Á.; Molés, F.; Peris, B. Analysis based on EU Regulation No 517/2014 of new HFC/HFO mixtures as alternatives of high GWP refrigerants in refrigeration and HVAC systems. *Int. J. Refrig.* **2015**, *52*, 21−31.

(16) Kamiaka, T.; Dang, C. B.; Hihara, E. Vapor-liquid equilibrium measurements for binary mixtures of R1234yf with R32, R125, and R134a. *Int. J. Refrig.* **2013**, *36* (3), 965−971.
(17) *ASHRAE ANSI/ASHRAE Standard 34-2019 Designation and Safety Classification of Refrigerants; American Society of Heating*, Refrigerating and Air-Conditioning Engineers: Atlanta, GA, 2019.
(18) Minor, B.; Spatz, M. *HFO-1234yf low GWP refrigerant update*, 2008.
(19) Karageorgis, A.; Hinopoulos, G.; Kim, M. H. A Comparative Study on the Condensation Heat Transfer of R-513A as an Alternative to R-134a. *Machines* **2021**, *9* (6), 114.
(20) Asensio-Delgado, S.; Viar, M.; Pardo, F.; Zarca, G.; Urtiaga, A. Gas solubility and diffusivity of hydrofluorocarbons and hydrofluoroolefins in cyanide-based ionic liquids for the separation of refrigerant mixtures. *Fluid Phase Equilib.* **2021**, *549*, 113210.
(21) Air-Conditioning, Heating, and Refrigeration Institute. *AHRI Standard 700-2019 Standard for Specifications for Refrigerants*; Air-Conditioning, Heating, and Refrigeration Institute: 2111 Wilson Boulevard, Suite 500, Arlington, VA 22201, USA, 2019.
(22) Nobuoka, K.; Kitaoka, S.; Iio, M.; Harran, T.; Ishikawa, Y. Solute-solvent interactions in imidazolium camphorsulfonate ionic liquids. *Phys. Chem. Chem. Phys.* **2007**, *9* (44), 5891−5896.
(23) Asensio-Delgado, S.; Viar, M.; Padua, A. A. H.; Zarca, G.; Urtiaga, A. Understanding the Molecular Features Controlling the Solubility Differences of R-134a, R-1234ze(E), and R-1234yf in 1-Alkyl-3-methylimidazolium Tricyanomethanide Ionic Liquids. *ACS Sustainable Chem. Eng.* **2022**, *10* (46), 15124−15134.
(24) Asensio-Delgado, S.; Pardo, F.; Zarca, G.; Urtiaga, A. Enhanced absorption separation of hydrofluorocarbon/hydrofluoroolefin refrigerant blends using ionic liquids. *Sep. Purif. Technol.* **2020**, *249*, 117136.
(25) Anthony, J. L.; Anderson, J. L.; Maginn, E. J.; Brennecke, J. F. Anion effects on gas solubility in ionic liquids. *J. Phys. Chem. B* **2005**, *109* (13), 6366−6374.
(26) Peng, D.; Robinson, D. B. A New Two-Constant Equation of State. *Ind. Eng. Chem. Fundam.* **1976**, *15* (1), 59−64.
(27) Mathias, P. M.; Klotz, H. C.; Prausnitz, J. M. Equation-of-State Mixing Rules for Multicomponent Mixtures - the Problem of Invariance. *Fluid Phase Equilib.* **1991**, *67*, 31−44.
(28) Valderrama, J. O.; Rojas, R. E. Critical Properties of Ionic Liquids. Revisited. *Ind. Eng. Chem. Res.* **2009**, *48* (14), 6890−6900.
(29) Sattari, M.; Kamari, A.; Mohammadi, A. H.; Ramjugernath, D. On the prediction of critical temperatures of ionic liquids: Model development and evaluation. *Fluid Phase Equilib.* **2016**, *411*, 24−32.
(30) Gardas, R. L.; Freire, M. G.; Carvalho, P. J.; Marrucho, I. M.; Fonseca, I. M. A.; Ferreira, A. G. M.; Coutinho, J. A. P. P rho T measurements of imidazolium-based ionic liquids. *J. Chem. Eng. Data* **2007**, *52* (5), 1881−1888.
(31) Rebelo, L. P. N.; Canongia Lopes, J. N.; Esperanca, J. M. S. S.; Filipe, E. On the critical temperature, normal boiling point, and vapor pressure of ionic liquids. *J. Phys. Chem. B* **2005**, *109* (13), 6040−6043.
(32) Ahrenberg, M.; Beck, M.; Neise, C.; Keßler, O.; Kragl, U.; Verevkin, S. P.; Schick, C. Vapor pressure of ionic liquids at low temperatures from AC-chip-calorimetry. *Phys. Chem. Chem. Phys.* **2016**, *18* (31), 21381−21390.
(33) Ge, R.; Hardacre, C.; Jacquemin, J.; Nancarrow, P.; Rooney, D. W. Heat capacities of ionic liquids as a function of temperature at 0.1 MPa. measurement and prediction. *J. Chem. Eng. Data* **2008**, *53* (9), 2148−2153.
(34) Shiflett, M. B.; Yokozeki, A. Solubility differences of halocarbon isomers in ionic liquid [emim] [Tf2N]. *J. Chem. Eng. Data* **2007**, *52* (5), 2007−2015.
(35) Asensio-Delgado, S.; Pardo, F.; Zarca, G.; Urtiaga, A. Vapor-Liquid Equilibria and Diffusion Coefficients of Difluoromethane, 1,1,1,2-Tetrafluoroethane, and 2,3,3,3-Tetrafluoropropene in Low-Viscosity Ionic Liquids. *J. Chem. Eng. Data* **2020**, *65* (9), 4242−4251.
(36) Sosa, J. E.; Ribeiro, R. P. P. L.; Castro, P. J.; Mota, J. P. B.; Araujo, J. M. M.; Pereiro, A. B. Absorption of Fluorinated Greenhouse Gases Using Fluorinated Ionic Liquids. *Ind. Eng. Chem. Res.* **2019**, *58* (45), 20769−20778.
(37) Sun, Y. J.; Di, G. L.; Wang, J.; Hu, Y. S.; Wang, X. P.; He, M. G. Gaseous solubility and thermodynamic performance of absorption system using R1234yf/IL working pairs. *Appl. Therm. Eng.* **2020**, *172*, 115161.
(38) Sun, Y. J.; Zhang, Y.; Wang, X. P.; Prausnitz, J. M.; Jin, L. W. Gaseous absorption of 2,3,3,3-tetrafluoroprop-1-ene in three imidazolium-based ionic liquids. *Fluid Phase Equilib.* **2017**, *450*, 65−74.
(39) Shiflett, M. B.; Yokozeki, A. Solubility and diffusivity of hydrofluorocarbons in room-temperature ionic liquids. *AIChE J.* **2006**, *52* (3), 1205−1219.
(40) Shiflett, M. B.; Yokozeki, A. Vapor-liquid-liquid equilibria of hydrofluorocarbons+1-butyl-3-methylimidazolium hexafluorophosphate. *J. Chem. Eng. Data* **2006**, *51* (5), 1931−1939.
(41) Zhang, Y.; Yin, J. J.; Wang, X. P. Vapor-liquid equilibrium of 2,3,3,3-tetrafluoroprop-1-ene with 1-butyl-3-methylimidazolium hexafluorophosphate, 1-hexyl-3-methyl imidazolium hexafluorophosphate, and 1-octyl-3-methylimidazolium hexafluorophosphate. *J. Mol. Liq.* **2018**, *260*, 203−208.
(42) Ren, W.; Scurto, A. M. Phase equilibria of imidazolium ionic liquids and the refrigerant gas, 1,1,1,2-tetrafluoroethane (R-134a). *Fluid Phase Equilib.* **2009**, *286* (1), 1−7.
(43) Liu, X. Y.; Bai, L. H.; Liu, S. Q.; He, M. G. Vapor-Liquid Equilibrium of R1234yf[HMIM] [Tf2N] and R1234ze(E)/[HMIM] [Tf2N] Working Pairs for the Absorption Refrigeration Cycle. *J. Chem. Eng. Data* **2016**, *61* (11), 3952−3957.
(44) Cao, Y. Y.; Mu, T. C. Comprehensive Investigation on the Thermal Stability of 66 Ionic Liquids by Thermogravimetric Analysis. *Ind. Eng. Chem. Res.* **2014**, *53* (20), 8651−8664.
(45) Ayuso, M.; Canada-Barcala, A.; Larriba, M.; Navarro, P.; Delgado-Mellado, N.; Garcia, J.; Rodriguez, F. Enhanced separation of benzene and cyclohexane by homogeneous extractive distillation using ionic liquids as entrainers. *Sep. Purif. Technol.* **2020**, *240*, 116583.
(46) Lek-utaiwan, P.; Suphanit, B.; Douglas, P. L.; Mongkolsiri, N. Design of extractive distillation for the separation of close-boiling mixtures: Solvent selection and column optimization. *Comput. Chem. Eng.* **2011**, *35* (6), 1088−1100.
(47) Gaurav, A.; Ng, F. T. T.; Rempel, G. L. A new green process for biodiesel production from waste oils via catalytic distillation using a solid acid catalyst - Modeling, economic and environmental analysis. *Green Energy Environ.* **2016**, *1* (1), 62−74.
(48) Ahosseini, A.; Ren, W.; Weatherley, L. R.; Scurto, A. M. Viscosity and self-diffusivity of ionic liquids with compressed hydrofluorocarbons: 1-Hexy1−3-methyl-imidazolium bis-(trifluoromethylsulfony)amide and 1,1,1,2-tetrafluoroethane. *Fluid Phase Equilib.* **2017**, *437*, 34−42.
(49) Crosthwaite, J. M.; Muldoon, M. J.; Dixon, J. K.; Anderson, J. L.; Brennecke, J. F. Phase transition and decomposition temperatures, heat capacities and viscosities of pyridinium ionic liquids. *J. Chem. Thermodyn.* **2005**, *37* (6), 559−568.
(50) Harris, K. R.; Kanakubo, M.; Woolf, L. A. Temperature and pressure dependence of the viscosity of the ionic liquids 1-hexyl-3-methylimidazolium hexafluorophosphate and 1-butyl-3-methylimidazolium bis(trifluoromethylsulfonyl)imide. *J. Chem. Eng. Data* **2007**, *52* (3), 1080−1085.
(51) Viar, M.; Asensio-Delgado, S.; Pardo, F.; Zarca, G.; Urtiaga, A. In the quest for ionic liquid entrainers for the recovery of R-32 and R-125 by extractive distillation under rate-based considerations. *Sep. Purif. Technol.* **2023**, *324*, 124610.

https://doi.org/10.1021/acs.iecr.3c03245
Ind. Eng. Chem. Res. 2023, 62, 19862−19872